第 25 卷第 11 期 无 机 化 学 学 报 Vol.25 No.11
2009 年 11 月 CHINESE JOURNAL OF INORGANIC CHEMISTRY 2040~2047

Ln 掺杂 $BiVO_4$(Ln=Eu、Gd、Er)光催化剂的制备和活性研究

张爱平* 张进治
(北方工业大学理学院,北京 100144)

摘要: 采用水热合成法, 制备出 Eu、Gd 和 Er 掺杂的 $BiVO_4$ 复合光催化剂,并采用 X 射线衍射、X 射线光电子谱、扫描电子显微镜和紫外–可见漫反射光谱技术对其进行分析表征。通过可见光下降解水溶液中甲基橙分子来考察其光催化性能,结果显示掺杂的复合光催化剂活性都强于纯的 $BiVO_4$,对掺杂复合光催化剂的催化活性增强机理进行了讨论和描述。

关键词: 光催化; 复合光催化剂; 可见光; 镧离子
中图分类号: O657.3 **文献标识码**: A **文章编号**: 1001-4861(2009)11-2040-08

Synthesis and Activities of Ln-Doped $BiVO_4$ (Ln=Eu, Gd and Er) Photocatalysts

ZHANG Ai-Ping* ZHANG Jin-Zhi
(*College of Sciences, North China University of Technology, Beijing* 100144)

Abstract: The Eu-, Gd- and Er-doped $BiVO_4$ composite photocatalysts were hydrothermal synthesized and characterized by X-ray diffraction, X-ray photoelectron spectroscopy, scanning electron microscopy and UV-Vis diffusion reflectance spectra techniques. Compared with the pure $BiVO_4$, all the composite photocatalysts exhibited the enhanced photocatalytic properties for degradation of methyl orange in aqueous solution under visible-light irradiation. The possible mechanism of the improvement in enhanced photocatalytic activity of composites was also discussed and schematized.

Key words: photocatalysis; composite photocatalyst; visible-light; lanthanide ions

0 Introduction

Bismuth vanadate ($BiVO_4$), one of the non-titania based visible-light-driven semiconductor photocatalysts[1,2], has recently attracted considerable attention for it′s commonly used as a photocatalyst in water splitting and oxidative decomposition of organic contaminants under visible-light irradiation[3~8]. Yet the photocatalytic activity of the pure $BiVO_4$ is not so strong due to its low quanta yield caused by the difficult migration of photogenerated electron-hole pairs[9~11]. As an efficient way to solve this problem, doping metal or metal oxide can always enhance the photocatalytic activities by separating the photogenerated electrons from holes.

Recently, Ag-$BiVO_4$ composites were prepared by Kohtani et al.[12] through an aqueous medium technique, and it showed superior visible-light activities than the pure $BiVO_4$ in decomposing long-chain alkylphenols and polycyclic aromatic hydrocarbons. Long et al.[13] reported that the Co_3O_4/$BiVO_4$ composite photocatalyst exhibited enhanced photocatalytic activity on degradation of phenol under visible-light irradiation. Xu et al.[14] found that the Cu-loaded $BiVO_4$ catalyst exhibited improved photocatalytic activity for the degradation of

收稿日期:2009-07-06。收修改稿日期:2009-08-21。
北京市教委面上科技项目(No.KM200910009011)资助。
*通讯联系人。E-mail:ncutalex@126.com;会员登记号:S060019227M。
第一作者:张爱平,男,26 岁,实验师;研究方向:光催化。

methylene blue; and the similar result had also been obtained by Jiang et al.[15]. Ge[16,17] prepared Pd/$BiVO_4$ by the impregnation method and demonstrated that it exhibited enhanced photocatalytic activities in decomposition of aqueous methyl orange under visible-light irradiation. Besides, other metals including Fe[10], Mn[18], Ce[19], W[20], Mo[21], V[22], Bi[23] and others doped in $BiVO_4$ had also been demonstrated to be effective in improving the photocatalystic activities of $BiVO_4$.

Although there have been many reports on transition metal and noble metal doping in $BiVO_4$, the effect of rare earth element doping on the photocatalytic activity of $BiVO_4$ for the organic contaminants photodegradation has seldom been reported so far as we know. However, other investigations showed that lanthanide ions/oxides with 4*f* electron configuration were better dopants in photocatalysts. El-Bahy et al. [24] reported that lanthanide ions (La^{3+}, Nd^{3+}, Sm^{3+}, Eu^{3+}, Gd^{3+} and Yb^{3+}) doped TiO_2 were synthesized by sol-gel method; and lanthanide ions can enhance the photocatalytic activity of TiO_2 for photodegradation of direct blue. Xie et al.[25] indicated that doping with Eu^{3+}, Nd^{3+} and Ce^{4+} can increase the photocatalytic degradation activities of TiO_2 catalysts in aqueous azo dye (X-3B) solution under visible-light irradiation. Therefore, using lanthanide element doped in catalysts could be an efficient way to increase the photocatalytic activity.

In this work, $BiVO_4$ was doped with different lanthanide element (Ln=Eu, Gd and Er) and characterized by XRD, XPS, SEM and DRS techniques. The influence of Ln doping on the photocatalytic decolorization of methyl orange was studied under visible-light irradiation. And the mechanism of the enhanced activity of Ln-$BiVO_4$ composite catalysts was also discussed.

1 Experimental

1.1 Synthesis of Ln-doped bismuth vanadate

In a typical preparation process[26], 0.02 mol $Bi(NO_3)_3\cdot 5H_2O$ and 0.02 mol NH_4VO_3 were dissolved separately in 20 mL of a 35% (*w*/*w*) HNO_3 and 20 mL of a 6 mol·L^{-1} NaOH solutions, individually, and each stirred for 30 min at room temperature. After that, these two mixtures were mixed together in a 1∶1 molar ratio and stirred for about 30 min to get a stable, salmon pink homogeneous solution. The same amount (0.5 g) of different lanthanide nitrate (including $Eu(NO_3)_3$, $Gd(NO_3)_3$ and $Er(NO_3)_3$) were then added into these solutions individually with a continuing stirring for 30 min to get the precursors. Mixture of each precursor were then sealed in a 50 mL Teflon-lined stainless autoclave and heated to 180 ℃ for 6 h under autogenous pressure. Afterwards, the precipitate was filtered, washed with distilled water three times for each, and dried in vacuum at room temperature for 12 h.

1.2 Apparatus and measurements

X-ray powder diffraction patterns (XRD, Puxi Co. LTD, model XD-3) were recorded in the region of 2θ= 10°~70° using Cu $K\alpha$ radiation (λ=0.154 18 nm) with a scan step of 2.0°·min^{-1} using a counter diffractometer. The morphologies and microstructures of as-prepared catalysts were examined using scanning electron microscopy (SEM, FEI Co., model Quanta-600). Energy-dispersive X-ray analysis (EDX) in the whole SEM was also taken for the chemical analysis of the doped catalysts. The BET special surface area of the catalysts was measured by N_2 adsorption at 77 K using a surface area detector (Jinaipu Co. LTD, model F-Sorb2400). X-ray photoelectron spectroscopy (XPS) analysis was performed on an X-ray photoelectron spectrometer (VG LIMS, model MKII) using the Mg Kα radiation. Optical absorbance spectra of the catalysts were obtained using a doubled-beam UV-Vis spectrophotometer (Puxi Co. LTD, model TU-1901) equipped with an integrating sphere. UV-Vis diffuse reflectance spectra (DRS) of $BiVO_4$ were recorded using $BaSO_4$ as a reference and were converted from reflection to absorbance by Kubelka-Munk method.

1.3 Photocatalytic activity test

Photocatalytic activities of the catalysts were determined by the decolorization of methyl orange (MO) under visible-light irradiation. A 500 W Xe-illuminator was used as a light source and set about 10 cm apart from the reactor. The 420 nm cutoff filter was placed between the Xe-illuminator and the reactor to completely remove all the incoming wavelengths shorter

than 420 nm to provide visible-light irradiation (λ>420 nm). Experiments were carried out at ambient temperature as follows: the same amount (0.2 g) of photocatalyst was added into 100 mL of a 10 mg·L^{-1} MO solution. Before illumination, the solution was stirred for 30 min in darkness in order to reach the adsorption-desorption equilibrium for MO and dissolved oxygen. At different irradiation time intervals, about 5 mL suspensions were collected, centrifugalized to remove the photocatalyst particles, and then used for the absorption tests. The concentrations of the remnant MO were monitored in the way of checking the absorbance of solutions at 464 nm during the photodegradation process.

2 Results and discussion

2.1 Powder formation

Fig.1 shows the XRD patterns of the pure $BiVO_4$ and Ln-loaded $BiVO_4$ series photocatalysts. It is confirmed that all the photocatalysts have a single monoclinic-scheelite structure, and no signals for any other phases or impurities were detected from the composite samples. The diffraction peaks of all samples are in conformity to the standard card of monoclinic $BiVO_4$ (PDF No.14-0688). This indicates that all the as-prepared photocatalysts have the same crystal structure. In addition, the obvious red shift of the peaks at about 18.6°, 18.9°, 28.9° and 30.5° corresponding to the (110), (011), (121) and (040) planes respectively were obtained, which may be caused by the doping of Ln^{3+} (Eu^{3+}, Gd^{3+} and Er^{3+}) ions in the composite catalysts. It is reported[27] that the base centered monoclinic $BiVO_4$ crystal (space group 15, *C*2/*c*) contains with the layered structure of Bi-V-O units. Since the radius of three lanthanide ions ($r(Eu^{3+})$=0.094 7 nm, $r(Gd^{3+})$=0.093 8 nm, and r (Er^{3+})=0.088 1 nm) are small than that of bismuth ion ($r(Bi^{3+})$=0.111 0 nm). Therefore, the lanthanide ions might enter into the lattice structure of $BiVO_4$ to replace Bi^{3+} ion, and thus lead to the shift of the diffraction peaks in their XRD patterns.

The high-resolution XPS analysis (Fig.2) was carried out to confirm the chemical states of Ln element in the composite catalysts. The Eu3*d*, Gd3*d* and Er3*d* XPS peaks were present at 1121.5, 1164.8, 1188.7, 1218.6, 1190.2 and 1121.3 eV, respectively. According to the literatures[25,26] and XPS peak-splitting analysis, it can be deduced that the Eu, Gd and Er elements in the photocatalysts are present as the form of their lanthanide oxide (Eu_2O_3, Gd_2O_3 and Er_2O_3, respectively).

Fig.3 shows the scanning electron microscopy (SEM) images of different catalysts; and their BET surface area data are listed in Table 1. In Fig.3a, the primary particle of the pure $BiVO_4$ showed small size (*ca.* 1~2 μm) and sintered significantly to each other to form the larger aggregates. In contrast, the dispersion of the composite catalysts was much higher than that of

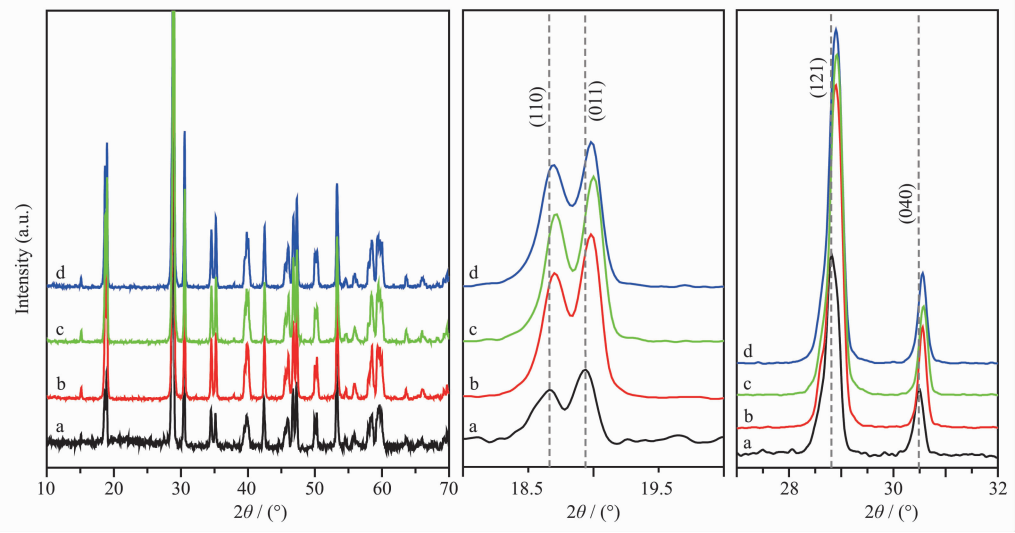

a: Pure $BiVO_4$, b: Eu-$BiVO_4$, c: Gd-$BiVO_4$, d: Er-$BiVO_4$

Fig. 1 XRD patterns of different catalysts

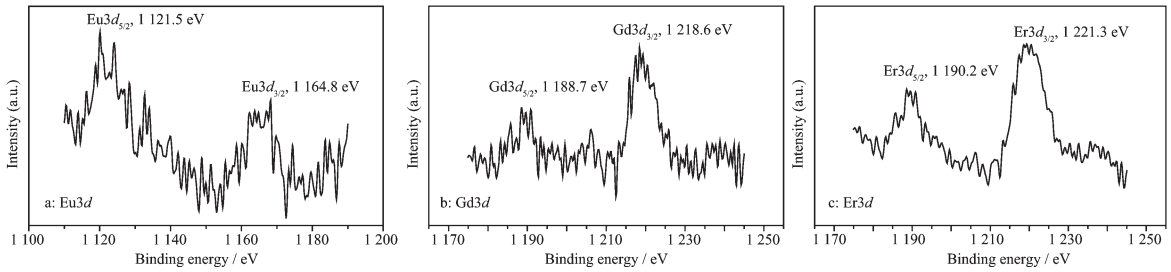

Fig.2　High-resolution XPS analysis of the doping element in different photocatalysts

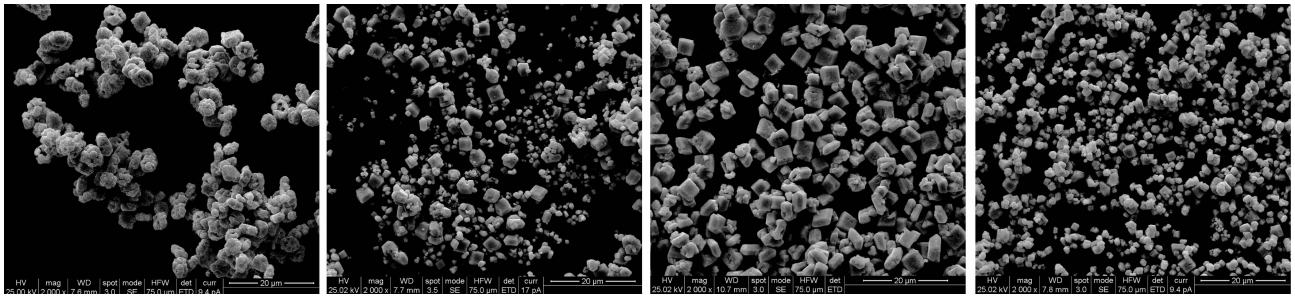

a: Pure $BiVO_4$　　b: Eu-$BiVO_4$　　c: Gd-$BiVO_4$　　d: Er-$BiVO_4$

Fig.3　SEM images of different catalysts

Table 1　Theoretical and experimental content of lanthanide element, BET surface areas of catalysts, MO equilibrium adsorption rate before irradiation and the total decolorize rate of dyes after 180 min irradation

Catalyst	Pure $BiVO_4$	Eu-$BiVO_4$	Gd-$BiVO_4$	Er-$BiVO_4$
Theoretical content / %	0.00	1.46	1.49	1.13
Experimental content / %	0.00	1.21	1.16	0.98
A_{BET} / ($m^2 \cdot g^{-1}$)	1.95	4.56	2.34	3.67
Adsorption rate / %	5.6	9.8	13.1	18.0
Total decolorize rate / %	13.7	98.1	88.7	99.4

the pure $BiVO_4$; and the composite catalysts showed high crystalline with smooth surface and plate form, which may lead to the improved photocatalytic activities. This is because the photocatalytic activity always gets higher with the increase of the catalyst crystallinity due to the suppressed recombination between photogenerated electrons and holes in highly crystalline photocatalysts[12,28]. The energy-dispersive X-ray analysis (EDX) studies (Fig.4) obtained from measurements at the whole SEM-micrograph, and it revealed that all the Ln-$BiVO_4$ composite catalysts had a homogenous atomic distribution with no other impure elements. This agrees well with the XRD and XPS results, and their EDX experimental data (Table 1) showed a little lower compared with the theoretical doping contents.

Fig.5 depicts UV-Vis diffuse reflectance spectra of different catalysts. As can be seen, the diffuse reflectance spectra of the composite catalysts have extended obvious red shifts in their edges and absorbance intensity increase in the visible range. These may be attributed to a charge transfer transition between the lanthanide ion and the energy bands of semiconductor[29]. For the yield of photogenerated electron-hole pair first depends on the intensity of incident photons with energy exceeding or equaling to the photocatalyst band gap energy, it thus indicated that the visible-light-responses of these Ln-$BiVO_4$ composite catalysts may be significantly improved by the lanthanide ion doping, and they should exhibit enhanced photoactivities than the pure $BiVO_4$ catalyst.

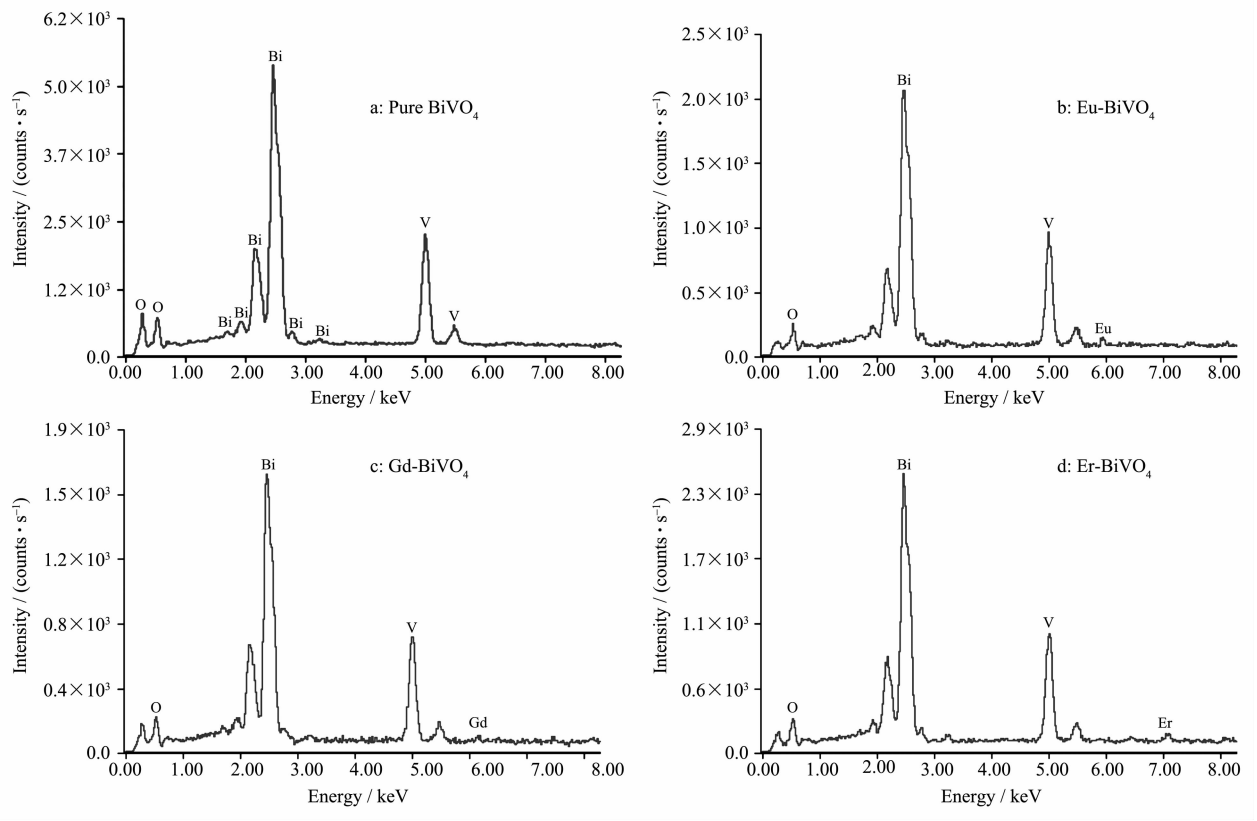

Fig.4 EDX spectra of different catalysts

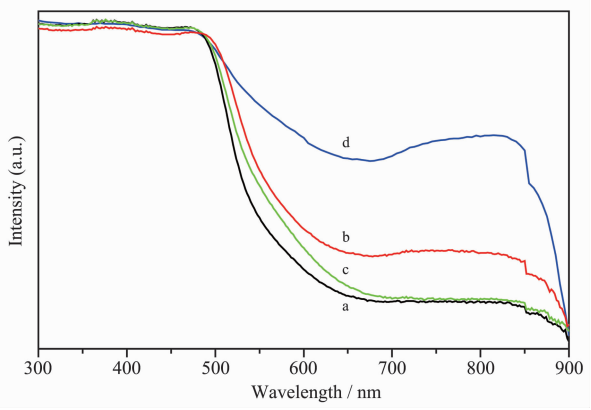

a: Pure $BiVO_4$, b: Eu-$BiVO_4$, c: Gd-$BiVO_4$, d: Er-$BiVO_4$

Fig.5 UV-Vis diffuse reflectance spectra of different catalysts

2.2 Photocatalyis activities

The changes in the absorption spectra of methyl orange (MO) aqueous solution during the photocatalytic process by the as-prepared catalysts at different irradiation time are shown in the inset of Fig.6. The decrease of absorption peaks at λ_{max}=465 nm in these figures indicates a degradation of MO molecules. For the pure $BiVO_4$ catalyst, the absorbance of MO at 465 nm decreased slowly after 180 min irradiation, and the total decolorize rate (including adsorption and photodegradation) of MO reached to 13.7%. This means that only a little part of the MO molecules in the solution had been decomposed. For the catalysts doped with Eu, Gd and Er, the photodegradation rates of MO had promptly reached 59.2%, 55.6% and 85.8% after only irradiating 90 min and reached up to 98.1%, 88.7% and 99.4% after irradiating 180 min, showing much higher activities than the pure $BiVO_4$ catalyst. In addition, the adsorption rates of the 10 mg·L^{-1} MO over pure $BiVO_4$ and Ln-doped $BiVO_4$ catalysts are also shown in Fig.6. After a stirring for 30 min in darkness to reach the adsorption-desorption equilibrium, the adsorption rate were 5.6%, 9.8%, 13.1% and 18.0% for the pure $BiVO_4$, Eu-, Gd- and Er-doped $BiVO_4$, respectively. Although the interfacial adsorption rate of Gd-doped $BiVO_4$ catalyst was higher than that of Eu-doped catalyst, the Gd-doped catalyst exhibited less decolorize rate than the Eu-doped $BiVO_4$. Thus, the improved interfacial adsorption abilities of the

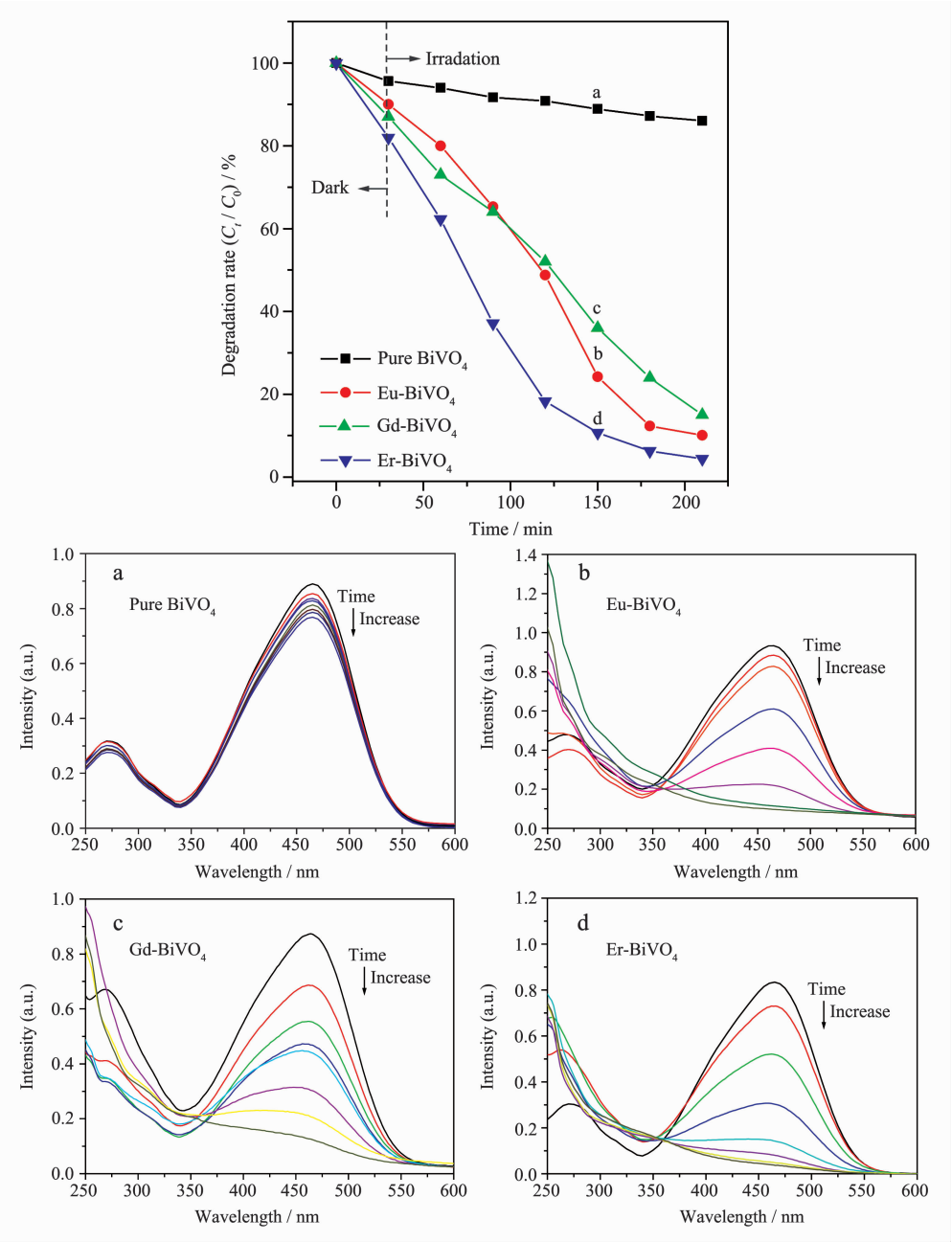

UV-Vis spectra profile changes of photocatalytic degradation of 10 mg·L^{-1} methyl orange by different catalysts at different irradiation times: (a) pure $BiVO_4$, (b) Eu-$BiVO_4$, (c) Gd-$BiVO_4$, (d) Er-$BiVO_4$

Fig.6　Comparison of the photocatalytic activities of different catalysts

composite catalysts were supposed to be only one of the reasons, but not the critical factor, for faster decomposition of dye molecules in these conditions.

2.3　Effects of Ln-doping on improved photocatalytic activities

As discussed above, the possible reasons for the enhanced photocatalytic of composite catalysts may be existed in the larger BET surface area for smaller particles with high dispersion and enhanced interfacial adsorption ability, the suppressed recombination between photogenerated electrons and holes in highly crystalline catalysts and the enhanced light absorption in the visible region, et al.

Since lanthanide element has partially-filled atomic f shell, the electrons at Ln^{3+} (Eu^{3+}, Gd^{3+} and Er^{3+}) 4*f* orbits could conduct electron-excitation and

electron-transition to build up lanthanide ions with a higher valence state by absorbing proper photons energy[29,30]. Consequently, surrounding Ln^{3+} ions may mutually bond due to self-sensitization and form positively-charged lanthanide ions cluster. This ions cluster had discrete empty multi-energy levels below the conduction band of crystalline $BiVO_4$. And their presence allowed a new electronic transition from the $BiVO_4$ valence band to the empty lanthanide ions cluster energy levels known as a sub-band gap with less energy than semiconductor valence-conduction band transition[31], as illustrated in Scheme 1.

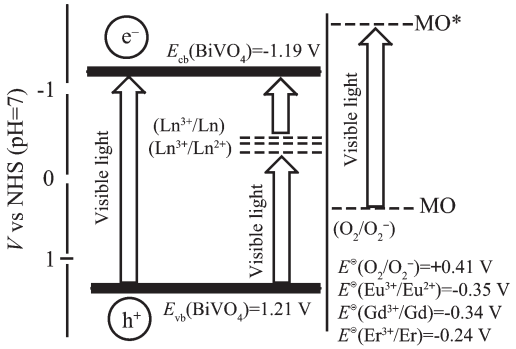

Scheme 1 Schematic illustration of valence and conduction band potentials of $BiVO_4$ along with the lanthanide ion pairs in the composite catalysts

On the other hand, the lanthanide ions doped in $BiVO_4$ particles could act as good scavengers to trap photoelectrons, leading to the separation of the photogenerated electrons from holes. According to the standard redox potentials of $E^\ominus(O_2/O_2)$=+0.41 V, $E^\ominus(Eu^{3+}/Eu^{2+})$=0.35 V[25], $E^\ominus(Gd^{3+}/Gd)$=0.34 V, $E^\ominus(Er^{3+}/Er)$=0.24 V[32] and $E_{vb}(BiVO_4)$=1.21 V versus NHE[13,27], the presence of Ln^{3+} ion on the $BiVO_4$ surface may promote the following reactions:

$$Ln^{3+}+3e^- \rightarrow Ln \quad or \quad Ln^{3+}+e^- \rightarrow Ln^{2+} \qquad (1)$$

$$Ln+3O_2 \rightarrow Ln^{3+}+3O_2^- \quad or \quad Ln^{2+}+O_2 \rightarrow Ln^{3+}+O_2^- \qquad (2)$$

It is generally believed that MO dye molecules can be excited under the visible-light illumination. The dye cationic radical (MO^+) produced by electron injection is less stable than the probe molecule in ground state. The excited state of dye molecule can inject electrons into the conduction band (CB) of $BiVO_4$ and may be trapped by the electron scavengers of surrounding oxygen molecule. In the meantime, it is also extremely susceptible for the recombination between cationic radicals and the electrons if the injection electrons accumulate in the CB of $BiVO_4$. So, the electrons trapping (Eq. (**1**)) and electrons transferring (Eq. (**2**)) reactions become two key steps to inhibit electron-cationic radical recombination. As a result, unstable dye cationic radicals can be directly degraded into its products by reacting with super-oxidizing anionic radials or other active oxygen[13]. In particular, the lanthanide ion doped in $BiVO_4$ plays an important role in promoting the electron trapping and electron transferring significantly in the dye/Ln-$BiVO_4$ system. The photosensitization reaction mechanisms in these systems can be illustrated in Scheme 2.

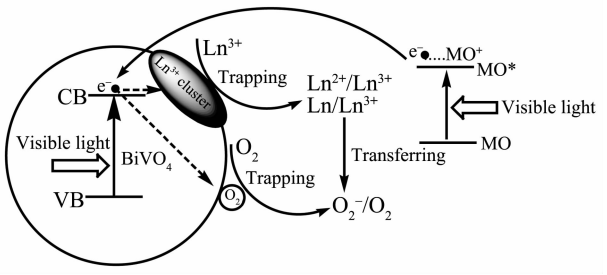

Scheme 2 Proposed photosensitization mechanism of dye/Ln-$BiVO_4$ systems under visible-light irradation

3 Conclusion

With attempts to improve the photocatalytic activity of $BiVO_4$ catalysts, three types of lanthanide ion-doped $BiVO_4$ catalysts (Ln-$BiVO_4$, Ln=Eu, Gd and Er) were prepared by hydrothermal method. The microstructures and morphologies of Ln-$BiVO_4$ catalysts were characterized by X-ray diffraction, X-ray photoelectron spectroscopy, scanning electron microscopy and UV-Vis diffusion reflectance spectra. It showed that the composite catalysts had better crystals and interfacial adsorption abilities than the pure $BiVO_4$ catalyst. The photocatalytic degradation of methyl orange (MO) in Ln-$BiVO_4$ reaction systems were studied to determine photocatalytic activities of the crystallized composite catalysts. And they all exhibited higher photocatalytic reactivities than the pure $BiVO_4$ catalyst significantly. Considering the electron-scavenging effect by Ln^{3+} ion, the mechanism of improved activities for

the composite catalysts was discussed and illustrated.

References:

[1] Xiao G C, Wang X C, Li D Z, et al. *J. Photoch. Photobio. A: Chem.*, **2008**,**193**:213~221

[2] Yu J Q, Kudo A. *Adv. Funct. Mater.*, **2006**,**16**:2163~2169

[3] Tücks A, Beck H P. *Dyes Pigments*, **2007**,**72**:163~177

[4] Lee J S. *Catal. Surv. Asia*, **2005**,**9**:217~227

[5] Zhou L, Wang W Z, Xu H L. *Cryst. Growth Des.*, **2008**,**8**:728~733

[6] LIU Jing-Bing(刘晶冰), WANG Hao(汪　浩), ZHANG Hui-Ming(张慧明), et al. *Chinese J. Inorg. Chem.*(*Wuji Huaxue Xuebao*), **2007**,**23**(7):1299~1302

[7] PENG Yang(彭　秧), HOU Lin-Rui(侯林瑞), YUAN Chang-Zhou(原长洲). *Chinese J. Appl. Chem.*(*Yingyong Huaxue*), **2008**,**25**(4):485~488

[8] GAO Shan-Min(高善民), QIAO Qing-An(乔青安), ZHAO Pei-Pei(赵培培), et al. *Chinese J. Inorg. Chem.*(*Wuji Huaxue Xuebao*), **2007**,**23**(7):1153~1158

[9] Gotic M, Music S, Ivanda M, et al. *J. Mol. Struct.*, **2005**,**744~747**:535~540

[10]Xu H, Li H, Wu C, et al. *Mater. Sci. Eng. B*, **2008**,**147**:52~56

[11]Guillodo M, Fouletier J, Dessemond L, et al. *J. European Ceramic. Soc.*, **2001**,**21**:2331~2344

[12]Kohtani S, Tomohiro M, Tokumura K, et al. *Appl. Catal. B: Environ.*, **2005**,**58**:265~272

[13]Long M, Cai W, Cai J, et al. *J. Phys. Chem. B*, **2006**,**110**:20211~20216

[14]Xu H, Li H, Wu C, et al. *J. Hazard. Mater.*, **2008**,**153**:877~884

[15]Jiang H, Endo H, Natori H, et al. *Mater. Res. Bull.*, **2009**,**44**:700~706

[16]Ge L. *Mater. Chem. Phys.*, **2008**,**107**:465~470

[17]Ge L. *Mater. Lett.*, **2008**,**62**:926~928

[18]Yang Y L, Qiu L, Harrison W T A, et al. *J. Mater. Chem.*, **1997**,**7**:243~248

[19]Neves M C, Lehocky M, Soares R, et al. *Dyes Pigments*, **2003**, **59**:181~184

[20]Chatchai P, Murakami Y, Nosaka A Y, et al. *Electrochimi. Acta*, **2009**,**54**:1147~1152

[21]Yao W, Iwai H, Ye J. *Dalton Trans.*, **2008**:1426~1430

[22]Jiang H, Nagai M, Kobayashi K. *J. Alloy Compd.*, **2009**,**24**:821~827

[23]Li L, Yan B. *J. Alloy Compd.*, **2008**,**476**:624~628

[24]El-Bahy Z M, Ismail A A, Mohamed R M. *J. Hazard. Mater.*, **2009**,**166**:138~143

[25]Xie Y, Yuan C, Li X. *Mater. Sci. Engin. B*, **2005**,**117**:325~333

[26]Zhang A, Zhang J, Cui N, et al. *J. Mol. Catal. A: Chem.*, **2009**, **304**:28~32

[27]Walsh A, Yan Y, Huda M N, et al. *Chem. Mater.*, **2009**,**21**:547~551

[28]Kudo A, Omori K, Kato H. *J. Am. Chem. Soc.*, **1999**,**121**:11459~11467

[29]Zhao D, Peng T, Liu M, et al. *Microporous Mesoporous Mater.*, **2008**,**114**:166~174

[30]Xu J, Ao Y, Fu D, et al. *J. Hazard. Mater.*, **2009**,**164**:762~768

[31]Wang Y, Takahashi K, Lee K H, et al. *Adv. Funct. Mater.*, **2006**,**16**:1133~1136

[32]Huheey J E. *Inorganic Chemistry*: *Principles of Structure and Reactivity* (*Third ed.*). New York: Harper & Row, **1983**.259~273